Vol. 729: 81–97, 2024
https://doi.org/10.3354/meps14500

MARINE ECOLOGY PROGRESS SERIES
Mar Ecol Prog Ser

Published February 22

Stable isotopes reveal that foraging strategy dictates trophic response of salt marsh residents to black mangrove *Avicennia germinans* range expansion

Katherine B. Loesser[1,*], Christina E. Powell[1,2,4], Brandeus Davis[1], Melissa M. Baustian[3,5], Michael J. Polito[1]

[1]Department of Oceanography and Coastal Sciences, Louisiana State University, Baton Rouge, LA 70803, USA
[2]Atkins, 920 Memorial City Way Suite 400, Houston, TX 77024, USA
[3]The Water Institute of the Gulf, Baton Rouge, LA 70802, USA

[4]*Present address:* Environmental Resources Management, Houston, TX 77024, USA

[5]*Present address:* US Geological Survey, Wetland and Aquatic Research Center, Baton Rouge, LA 70808, USA

ABSTRACT: Climate warming has facilitated the expansion of black mangrove *Avicennia germinans* (hereafter '*Avicennia*') into smooth cordgrass *Spartina alterniflora* (hereafter '*Spartina*') salt marshes in southeastern Louisiana (USA). As macrophytes contribute to soil organic matter (SOM) and primary production, this transition could alter the basal energy pathways supporting salt marsh food webs. We used bulk-tissue and compound-specific stable isotope analyses (SIA) to determine if changes in dominant macrophytes alter basal energy pathways for 2 salt marsh residents: grass shrimp (*Palaemonetes* spp.) and marsh periwinkle snails *Littoraria irrorata*. Specifically, we used Bayesian stable isotope mixing models to quantify the relative contribution of basal energy sources to SOM and resident food webs across a *Spartina*–*Avicennia* gradient in southeastern Louisiana. We found that sources of SOM changed in *Avicennia*-dominated habitat and that foraging strategy dictated trophic responses of salt marsh residents to *Avicennia* expansion. Marsh periwinkle snail basal energy sources shifted from *Spartina* to algae (phytoplankton and epiphytic macroalgae) reliance, while grass shrimp basal energy sources remained reliant on algal production, regardless of macrophyte dominance. Compound-specific SIA improved basal energy source distinctions and provided more constrained estimates of their contributions to resident food webs than bulk-tissue SIA. The importance of algal energy across the landscape warrants future investigations into the ability of *Avicennia* to support the diversity and abundance of algal energy sources present in Louisiana salt marshes. Understanding coastal wetland food web dynamics could help with planning and evaluating the most effective coastal restoration techniques (e.g. prioritizing salt marsh or mangrove habitat) in southeastern Louisiana.

KEY WORDS: Stable isotope · *Avicennia germinans* · *Spartina alterniflora* · Climate change · Food web · *Littoraria irrorata* · *Palaemonetes* spp. · Amino acid

1. INTRODUCTION

In the northern Gulf of Mexico, black mangroves *Avicennia germinans* (hereafter '*Avicennia*') are expanding into smooth cordgrass *Spartina alterniflora* (also known as *Sporobolus alterniflorus*; hereafter '*Spartina*') dominated salt marshes. While spurred by natural processes (e.g. Earth eccentricity, obliquity, and precession), this poleward expansion is accelerated by anthropogenic climate warming (Rodrigues et al. 2021) and the resulting decreased frequency of extreme freeze events (Osland et al.

*Corresponding author: ktboole@gmail.com

2013, Cavanaugh et al. 2014, Osland et al. 2020). Southeastern Louisiana is near the northern limit of this expansion and includes nearly 40% of all salt marshes in the contiguous USA (Day et al. 2012). *Avicennia* outcompetes *Spartina* in the northern hemisphere (Guo et al. 2013, Osland et al. 2013), so an eventual shift in dominant wetland macrophyte is likely. Given their differences in morphology (i.e. shrub-like tree vs. grass), this shift could significantly affect ecosystem structure and function in this region (Osland et al. 2013, Cavanaugh et al. 2014, Smee et al. 2017, Scheffel et al. 2018).

Mangroves provide increased storm protection (Comeaux et al. 2012) while matching the ability of *Spartina* to mitigate sea level rise (McKee & Vervaeke 2018) and store carbon (Yando et al. 2016). Yet, little is known about the food web consequences of a transition from salt marsh to mangrove habitat. Salt marsh food web energy pathways are complex, as *Spartina* can be a significant basal energy source on its own (Winemiller et al. 2007) or in combination with phytoplankton, epiphytic macroalgae, and/or microphytobenthos (hereafter 'algae'; Currin et al. 1995, Abrantes et al. 2015). There is growing evidence of the importance of algae for provisioning energy to salt marsh food webs (e.g. Alderson et al. 2013, Baker et al. 2021), but the relative importance of *Spartina* versus algae varies by site and consumer species (Deegan & Garritt 1997, Deegan et al. 2002, Abrantes et al. 2015). In contrast, mangrove carbon inputs to tropical mangrove forest food webs are often minimal, with algae consistently serving as the most critical basal energy source for consumers (Alfaro 2008, Henriques et al. 2021, Harada et al. 2022). In addition to directly provisioning energy, *Spartina* facilitates the presence of other crucial basal energy sources by contributing detritus to soil organic matter (SOM; Haines 1976), outwelling nitrogen to phytoplankton (Whiting et al. 1989, Fry 2006), and providing a substrate for epiphytic macroalgal growth (Sullivan 1982). Because the capacity of *Avicennia* to provide these same functions is unknown, replacing *Spartina* with *Avicennia* could directly and/or indirectly affect energy pathways in salt marsh food webs.

Previous studies investigating the food web effects of this shift in the southeastern USA have used bulk-tissue stable isotope analysis (SIA) and isotopic mixing models to quantify basal energy pathways supporting consumers. For instance, along the eastern Florida coast, algae contributions to consumers in coastal wetlands exceed both *Spartina* and mangrove contributions regardless of which macrophyte is dominant; however, detrital pathway-associated species (e.g. fiddler crabs [*Uca* spp.], grass shrimp [*Palaemonetes* spp.], and mullet *Mugil cephalus*) demonstrate some reliance on *Spartina* energy, when present (Baker et al. 2021). Similarly, in southeastern Louisiana, algal production (i.e. phytoplankton/particulate organic matter and epiphytic macroalgae) is the primary energetic support for nektonic species in coastal wetland food webs, irrespective of macrophyte dominance patterns (Nelson et al. 2019). Importantly, *Spartina* contributes to these food webs in southeastern Louisiana, but *Avicennia* does not. While Nelson et al. (2019) focused exclusively on salt marsh nekton and extensively on transient species (i.e. those that only spend a portion of their life cycle within the marsh complex), deposit-feeding and/or resident species (i.e. those that spend their entire life cycle within the marsh complex) may have a greater sensitivity to *Avicennia* expansion (Guest & Connolly 2005).

Many salt marsh residents exhibit diverse foraging strategies, including nektonic grazers, like grass shrimp (*Palaemonetes* spp.), and epibenthic deposit feeders, like marsh periwinkle snails *Littoraria irrorata* (hereafter 'periwinkles'). Both of these species can be detrital pathway-associated (Welsh 1975, Treplin et al. 2013) and prey for important fisheries species (e.g. red drum *Sciaenops ocellatus* and blue crab *Callinectes sapidus*; Anderson 1985, McQuaid 1996). Grass shrimp primarily graze on epiphytic microalgae and meiofauna growing on *Spartina* stems (Gregg & Fleeger 1998, Fleeger et al. 1999) and, as nekton, have high mobility across salt marsh sub-habitats (Kneib 2002). Periwinkles are *Spartina*-detritus specialists (Silliman & Newell 2003, Sieg et al. 2013), extensively graze marsh sediment (Alexander 1979), and have narrow home ranges restricted to the marsh platform (Vaughn & Fisher 1992). Given the potential vulnerability of salt marsh residents following a loss of *Spartina* in southeastern Louisiana, the food web effects of *Avicennia* expansion on these consumers is an important aspect to fully assess.

Bulk-tissue SIA can be a valuable tool for estimating basal energy source contributions to salt marsh consumers, but it has several limitations. Tissue values of consumers can be influenced by internal biosynthesis, obscuring true basal energy source values, and the relative contributions of terrestrial and aquatic energy sources can also be difficult to distinguish (Johnson et al. 2019). As such, isotopic mixing models using bulk-tissue SIA often have high degrees of posterior overlap, making it difficult to fully tease apart the importance of different energy sources (e.g. Baker et al. 2021). Compound-specific

stable isotope analysis (CSIA) measures the stable isotope ratios of individual molecules (e.g. amino acids, CSIA-AA). CSIA-AA applied to essential amino acids (EAAs) can help reduce the confounding effect of internal biosynthesis and provides more axes of variation to discriminate basal energy sources, particularly improving the distinction between dominant macrophytes and algae (Johnson et al. 2019). Yet, CSIA-AA is costly, so determining how much more interpretive power it provides relative to bulk-tissue SIA is worthwhile.

The purpose of this study was to explore the food web effects of *Avicennia* expansion into *Spartina*-dominated salt marshes in southeastern Louisiana. We aimed to determine if changes in the dominant macrophyte alter SOM and/or the basal energy pathways supporting resident salt marsh consumers. Our specific objectives were to use SIA to determine the relative contribution of basal energy sources to (1) SOM and (2) resident salt marsh consumers (grass shrimp and periwinkles) in *Spartina*-dominated, mixed, and *Avicennia*-dominated wetland habitat. We then aimed to (3) compare the effectiveness of bulk-tissue SIA and CSIA-AA in estimating basal energy source contributions to these 2 consumers along this *Spartina*—*Avicennia* habitat gradient. We expected that the basal carbon composition of SOM across habitats would reflect macrophyte abundance and that basal energy sources supporting grass shrimp food webs would agree with previous findings (i.e. high reliance on labile algae across habitats; Nelson et al. 2019). In contrast, we expected that basal energy sources supporting periwinkle food webs would shift in response to changing macrophyte dominance due to a close association with *Spartina*, deposit-feeding strategy, and limited mobility. Last, we expected that CSIA-AA would provide a more precise (i.e. less variable and more differentiated across sources) assessment of consumers' basal energy source use in all species and habitats, similar to a recent study of another common saltmarsh species, the seaside sparrow *Ammodramus maritimus* (Johnson et al. 2019).

2. MATERIALS AND METHODS

2.1. Study site

This study focused on back barrier saline marshes of Grand Isle, Louisiana, located within the westernmost portion of Barataria Basin in southeastern Louisiana (Fig. 1). Barataria Basin lies within the Mississippi River Deltaic Plain, but direct riverine inputs are minimal due to the channelization of the Mississippi River (Alexander et al. 2012). The Basin is separated from the Gulf of Mexico by a series of barrier islands, and its saline wetlands primarily consist of *Spartina*-dominated salt marshes. *Avicennia* has been observed in the Basin since the early 1700s but has increased in prevalence over time (Osland et al. 2020). It currently co-exists within saline marshes, interspersed with *Spartina*, forming a mosaic of *Spartina*-dominated patches, mixed patches, and *Avicennia*-dominated patches (Rodrigues et al. 2021). As a microtidal system, climatological factors (e.g. wind, precipitation) predominantly influence Basin hydrology and salinity (Childers et al. 1990, Conner & Day 1987).

2.2. Sample collection

We collected samples on 23 May 2015, from 3 adjacent wetland sites representing *Spartina*-dominated (29.2294° N, 90.0086° W), mixed (29.2288° N, 90.0142° W), and *Avicennia*-dominated habitat (29.2286° N, 90.0133° W; hereafter marsh, mixed, and mangrove habitat, respectively; Fig. 1). During the year of sample collection, salinity in the study area ranged from 3.43 to 26.62, with an average and standard deviation (SD) of 15.43 ± 5.30, and water temperature ranged from 6.75 to 35.18°C, with an average and SD of 23.34 ± 6.42°C (Station CRMS0178; Coastal Protection and Restoration Authority 2015). We initially selected each site area based on the spatial coverage and shoreline expanse of monoculture or vegetation mixture. Of the total vegetation present (i.e. excluding bare sediment), the dominant sites had approximately 75% or greater coverage by the dominant species, and the mixed site had approximately 50% coverage of each. Within each site, we collected macrophyte and SOM samples from 5 randomly assigned 0.25 m^2 plots. These plots had approximately 100% coverage of the dominant macrophyte in dominant sites and approximately 50% coverage of each macrophyte in the mixed site.

Basal energy sources included live *Spartina* leaves, live *Avicennia* leaves, and a phytoplankton and particulate organic matter (POM) proxy (ribbed mussels *Geukensia demissa*; Post 2002), collected by hand (see Table 1). We collected SOM using a small push core (3 cm diameter, 5 cm length) immediately adjacent to or beneath plants. We collected grass shrimp (n = 30) and periwinkles (n = 30) by dip net and by hand, respectively. All samples were analyzed for

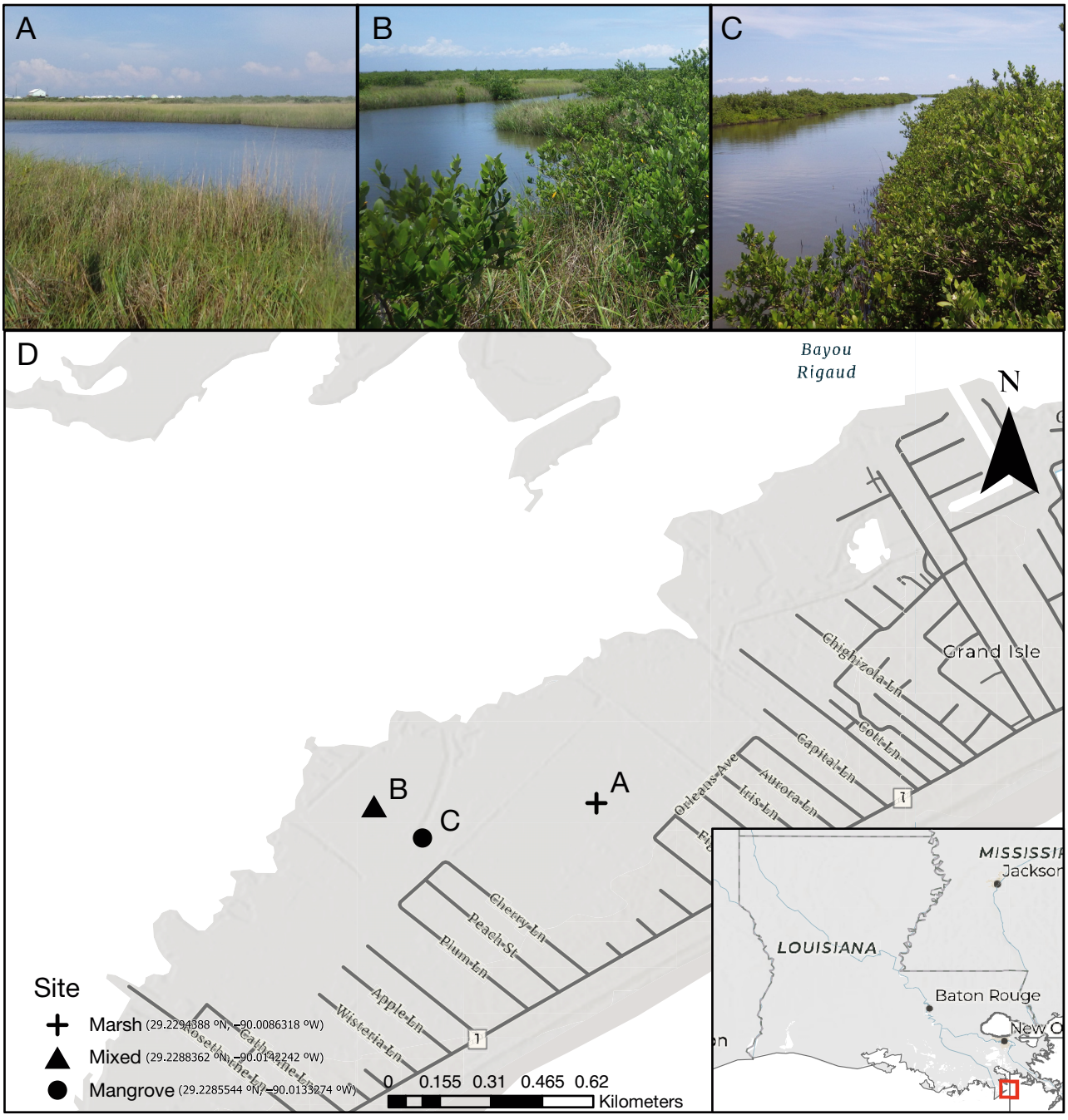

Fig. 1. Location of (A) *Spartina*-dominated (marsh), (B) mixed, and (C) *Avicennia*-dominated (mangrove) sites on (D) Grand Isle, Louisiana, USA. Created using ArcGIS software (Esri). Photographs by Melissa M. Baustian

bulk-tissue $\delta^{13}C$ and $\delta^{15}N$ values, and a subset was analyzed for CSIA-AA $\delta^{13}C$ values (see Table 2).

To supplement these collections, we compiled published data sets for epiphytic macroalgae collected in lower Barataria Bay. Specifically, we gathered bulk-tissue $\delta^{13}C$ and $\delta^{15}N$ values reported by Nelson et al. (2019) for epiphytic macroalgae collected from macrophyte stems and roots by physically removing material near Port Fourchon, Louisiana (29.10° N, 90.19° W) in August–September 2016. We also obtained CSIA-AA $\delta^{13}C$, % carbon, and % nitrogen values reported by Moyo et al. (2020) for epiphytic macroalgae collected from macrophyte stems near Port Sulphur, Louisiana (29.5155° N, 89.7880° W) in May 2016.

2.3. Sample processing

We dried plant and SOM samples in an oven at 60°C for 48 h and then removed roots and other large pieces of vegetation from the SOM. We dissected mussel, grass shrimp, and periwinkle specimens to isolate muscle tissue, which was lyophilized for 24 h. All samples were ground into a homogenized powder using a ball mill (Crescent Wig-L-Bug, DENTSPLY Rinn) for plants and a mortar and pestle for SOM and muscle tissue. We extracted lipid from muscle samples using a 2:1 chloroform:methanol solution following a modification of Kim & Koch (2012) that did not include rinsing with deionized water, as this step is used to remove uric acid that is unique to elasmobranch samples.

2.4. Bulk-tissue SIA

We weighed approximately 4 mg of each plant sample, 10–40 mg of each SOM sample, and 0.5–0.7 mg of each muscle sample into tin capsules for bulk-tissue $\delta^{13}C$ and $\delta^{15}N$ analysis. We then flash-combusted these samples using an ECS4010 elemental analyzer (Costech) coupled to a Delta Plus XP (Thermo-Fisher Scientific) continuous-flow isotope ratio mass spectrometer (IRMS) to measure carbon and nitrogen stable isotope abundances at Louisiana State University (Baton Rouge, Louisiana, USA). We used glutamic acid (USGS-40 and USGS-41), sorghum flour (SKU B2158, EA Consumables), and wheat flour (SKU B2156, EA Consumables) certified reference materials to normalize raw stable isotope values on a 2-point scale. Stable isotope abundances were expressed in delta notation (δ) and per mil units (‰) using the following equation, where X is ^{13}C or ^{15}N and R is the respective atomic ratio of heavy to light isotopes (i.e. ^{13}C:^{12}C or ^{15}N:^{14}N):

$$\delta X = \left[\left(R_{\text{sample}} - R_{\text{standard}}\right) - 1\right] \times 1000 \quad (1)$$

R_{standard} values were derived from Vienna PeeDee Belemnite for $\delta^{13}C$ and atmospheric nitrogen gas for $\delta^{15}N$. Sample precision was 0.1‰ for $\delta^{13}C$ and 0.2‰ for $\delta^{15}N$ based on repeated reference materials.

2.5. CSIA

We weighed approximately 30 ± 0.025 mg of each plant sample and 2 ± 0.025 mg of each muscle sample into 4.0 ml glass vials for CSIA-AA $\delta^{13}C$ of the 5 EAAs detectable with our instrumentation: isoleucine (Ile), leucine (Leu), phenylalanine (Phe), threonine (Thr), and valine (Val). Before CSIA-AA, we acid-hydrolyzed samples in 6N HCl (2 ml for plants, 1 ml for muscle), flushed with nitrogen gas, at 110°C for 20 h to break proteins into individual amino acids. Following hydrolysis, we dried samples at 65°C under a stream of nitrogen gas. To remove excess particulates, we columned plant samples using a Dowex 50WX8-400 cation exchange resin following Metges et al. (1996). Immediately preceding analysis, we volatilized amino acids by resuspending samples in 100 µl of L-norleucine solution and derivatizing them with a methyl chloroformate-based method, following Walsh et al. (2014).

We injected CSIA-AA samples in splitless mode at 250°C and separated them on an Agilent J&W VF-23 ms column (30 m long, 0.25 mm outer diameter, 0.25 mm film thickness) in a Trace 1310 GC gas chromatograph (Thermo-Fisher Scientific). We combusted separated amino acids at 1000°C and measured them for isotope abundances using a Delta V Advantage IRMS (Thermo-Fisher Scientific). We used L-norleucine as an internal standard to calculate provisional values for each sample. Raw values reported in delta notation (δ) and per mil units (‰) were corrected for non-analyte carbon and kinetic isotope effects using a reference material with amino acids of known isotopic value (L-AA mix; Docherty et al. 2001). We measured this reference material at a range of concentrations to allow for linearity corrections using a linear model (Werner & Brand 2001, Reinnicke et al. 2012) and after every fourth injection to allow for drift corrections using a logarithmic model (Werner & Brand 2001, Reinnicke et al. 2012). We included 3 additional internal standard reference materials (D-AA mix, Atlantic cod *Gadus morhua*, and red drum *Sciaenops ocellatus* muscle tissues) for instrument precision quality assurance. Sample precision across all 5 EAAs was ±0.21‰ for $\delta^{13}C$.

2.6. SOM bulk-tissue mixing models

To assess if SOM composition differs with changes in dominant macrophytes, we first used ANOVA followed by Tukey's honestly significant difference (HSD) test to determine if there was a statistically significant ($p < 0.05$) difference in SOM bulk-tissue $\delta^{13}C$ and $\delta^{15}N$ values across habitats. For all ANOVA and Tukey's HSD tests here and below, data and residuals were plotted to confirm homogeneity of variance and normality in residual distributions. SOM had significantly lower mean $\delta^{13}C$ values in mangrove habitat than in marsh or mixed habitats ($p < 0.05$; Table 1). We then incorporated bulk-tissue isotope

Table 1. Mean ± SD $\delta^{13}C$ values, $\delta^{15}N$ values, percent carbon (% C), and percent nitrogen (% N) of basal energy sources, soil organic matter, and consumers. Source values in **bold** were used in mixing models along with individual consumer estimates. The phytoplankton/particulate organic matter (POM) proxy and epiphytic macroalgae were combined *a posteriori* in the mixing models. Sampling limitations prevented the collection of mussels and macroalgae from all 3 habitat types. Superscript letters indicate statistically significant ($p < 0.05$) basal energy source groupings based on Tukey's honestly significantly difference test. ⋆Epiphytic macroalgae values from Nelson et al. (2019). †Epiphytic macroalgae % C and % N from Moyo et al. (2020)

	Species	Habitat	n	$\delta^{13}C$ (‰)	$\delta^{15}N$ (‰)	% C	% N
Basal energy sources	Saltmarsh cordgrass *Spartina alterniflora*	Marsh	5	−13.6 ± 0.5	5.0 ± 0.6	37.6 ± 8.3	1.0 ± 0.3
		Mixed	5	−13.3 ± 0.5	5.1 ± 1.0	40.9 ± 0.8	0.9 ± 0.2
		Total	10	**–13.5^{a} ± 0.5**	**5.1^{a} ± 0.7**	**39.3** ± 5.8	**1.0** ± 0.3
	Black mangrove *Avicennia germinans*	Mixed	5	−24.9 ± 0.8	3.8 ± 0.7	45.4 ± 0.5	1.6 ± 0.2
		Mangrove	6	−28.3 ± 2.1	4.05 ± 0.3	42.0 ± 2.3	1.6 ± 0.2
		Total	11	**–26.7^{b} ± 2.4**	**3.9^{b} ± 0.5**	**43.6** ± 2.4	**1.6** ± 0.2
	Ribbed mussel *Geukensia demissa* — POM proxy	Marsh	9	−19.9 ± 0.3	9.2 ± 0.3	43.5 ± 0.7	14.3 ± 0.4
		Mixed	10	−20.4 ± 0.6	8.2 ± 0.3	43.3 ± 0.9	13.8 ± 0.6
		Total	19	**–20.1^{c} ± 0.5**	**8.7^{c} ± 0.6**	**43.4** ± 0.8	**14.0** ± 0.6
	Epiphytic macroalgae⋆	Marsh	4	−19.6 ± 1.9	5.1 ± 0.9	—	—
		Mangrove	5	−20.9 ± 1.2	5.4 ± 1.0	—	—
		Total	9	**–20.3^{c} ± 1.9**	**5.3^{a} ± 0.9**	**24.8** ± 3.5†	**2.8** ± 0.6†
Soil organic matter		Marsh	5	**−17.7^{d} ± 0.9**	**3.4^{bd} ± 0.5**	**8.0** ± 1.4	**0.6** ± 0.1
		Mixed	5	**−18.4^{cd} ± 0.7**	**2.6^{d} ± 0.7**	**8.9** ± 3.0	**0.6** ± 0.2
		Mangrove	5	**−24.9^{b} ± 1.9**	**3.7^{bd} ± 0.5**	**4.0** ± 1.9	**0.3** ± 0.1
Consumers	Grass shrimp (*Palaemonetes* spp.)	Marsh	10	−17.9 ± 0.8	9.3 ± 0.6	43.5 ± 2.7	13.9 ± 0.8
		Mixed	10	−17.7 ± 1.8	8.9 ± 1.0	44.3 ± 2.7	14.1 ± 0.3
		Mangrove	10	−18.1 ± 1.0	8. 9 ± 0.6	42.7 ± 1.8	13.7 ± 0.6
	Marsh periwinkle snail *Littoraria irrorata*	Marsh	10	−13.9 ± 0.6	8.1 ± 0.4	39.3 ± 3.4	11.4 ± 1.6
		Mixed	10	−13.8 ± 0.7	7.8 ± 0.4	42.7 ± 12.3	12.3 ± 3.7
		Mangrove	10	−20.4 ± 0.7	5.4 ± 0.8	39.0 ± 2.7	10.9 ± 1.6

data into a single-tracer ($\delta^{13}C$) mixing model to estimate the proportional contributions of each basal carbon source (*Spartina*, *Avicennia*, the POM proxy, and epiphytic macroalgae) to SOM from each habitat (marsh, mixed, and mangrove) using the 'simmr' package (Parnell 2021) in R Version 4.0.3 (R Core Team 2020). We averaged basal carbon sources across sampled habitats and considered all as possible end members for each SOM sample, even if uncommon in a specific habitat (i.e. *Spartina* in mangrove habitats or *Avicenna* in marsh habitats), due to the proximity of sites and high connectivity of estuarine systems, which facilitates organic matter transport from adjacent areas (Fagherazzi et al. 2013). An ANOVA with Tukey's HSD test on basal carbon sources indicated that the POM proxy and epiphytic macroalgae did not significantly differ in $\delta^{13}C$ (Table 1), so we combined them into an 'algae' source *a posteriori* (Phillips et al. 2014), resulting in 3 basal carbon sources for the mixing model.

We applied a trophic enrichment factor (TEF) of zero with a minimal SD (0.3‰) to this model, assuming little to no isotopic fractionation between basal carbon sources and SOM (Klink et al. 2022). We plotted TEF-adjusted mean basal carbon source bulk-tissue δ values and all SOM bulk-tissue δ values to ensure that sources adequately captured SOM variability before proceeding with the mixing model (Fig. 2A; Phillips et al. 2014). The model generated 4 Markov chains of 10 000 iterations each, discarded the first 1000 iterations as burn-in, and thinned by 10, resulting in 3600 total posterior data points for each parameter. We evaluated parameter convergence using the Gelman-Rubin diagnostic and visualization of the posterior predictive distribution (Gelman 2004). We compared basal carbon source contributions to SOM within and across habitats using the overlap of 95% credible intervals (CIs) and pairwise comparisons of the model's posterior predictive distributions. Specifically, we used the 'compare_sources'

and 'compare_groups' functions (Parnell 2021), respectively, to determine the posterior probability (PP) that a given basal carbon source constituted a greater proportion of SOM carbon than another source within a given habitat, and the PP that a given source constituted a greater proportion of SOM in one habitat relative to another habitat. This Bayesian probabilistic interpretation approach allows for understanding the magnitude of certainty surrounding an effect rather than imposing the binary outcome significance or insignificance common to frequentist or other estimation routines.

2.7. Consumer bulk-tissue SIA mixing models

To assess if the basal energy sources supporting consumers differ with changes in dominant macrophytes, we first used a 2-way ANOVA (with interaction) followed by Tukey's HSD to evaluate the effect of consumer species and habitat on bulk-tissue $\delta^{13}C$ and $\delta^{15}N$ values. There were no significant differences for grass shrimp across habitats, but periwinkles in the mangrove habitat significantly differed from those in the marsh and mixed habitats for both tracers ($p < 0.05$; Table 1). We then incorporated bulk-tissue stable isotope data into 2-tracer ($\delta^{13}C$ and $\delta^{15}N$) mixing models ($n = 6$) to estimate the proportional contributions of each basal energy source (*Spartina*, *Avicennia*, the POM proxy, epiphytic macroalgae) and SOM to each consumer group separately (grass shrimp and periwinkles from marsh, mixed, and mangrove habitats, respectively). We averaged basal energy sources as described above, but we used habitat-specific SOM δ values, as it was collected from all habitats, and isotopic composition varied accordingly (Table 1). As with the SOM bulk-tissue mixing model, we combined the POM proxy and epiphytic macroalgae into an 'algae' source *a posteriori*. The remaining basal energy sources were statistically distinct for at least 1 tracer, except for *Avicennia* and SOM from the mangrove habitat (Table 1). Even so, we kept *Avicennia* and SOM separate in mangrove habitat models to keep the number of basal energy sources consistent across all models.

We used a base TEF of 0.9 ± 0.3‰ for carbon and 2.9 ± 0.5‰ for nitrogen following Nelson et al. (2019). We then calculated the trophic position of grass shrimp (2.48) and periwinkles (2.00) using the 'NetIndices' package in R (Kones et al. 2009), based on the diet matrix of McCann et al. (2017). We subsequently multiplied the base TEF by each species' trophic step, the difference between its trophic level and the source trophic level, to derive species-specific TEFs following Hernandez et al. (2021). We plotted TEF-adjusted mean basal energy source bulk-tissue δ values and all consumer bulk-tissue δ values to ensure sources adequately captured consumer variability before proceeding with mixing models (Fig. 2B,C; Phillips et al. 2014).

Because SOM is a complex mixture of basal energy sources, the contributions of which were estimated following the above, we reallocated SOM contribution to the 3 basal energy sources using the SOM mixing model results. Specifically, we reallocated SOM proportional estimates for each posterior data point using the posterior data points generated in the SOM mixing model. This allowed a more direct comparison to the CSIA-AA mixing model and more directly addressed the study's goal of determining the degree to which *Avicennia* supports salt marsh consumers following habitat transition. Model specifications (i.e. number of chains, iterations, burn-in, and thinning) were as described above. Additionally, we used the same metrics for evaluating parameter convergence (i.e. Gelman-Rubin diagnostic, posterior predictive distribution visualization) and comparing consumer model outputs within and across habitats (i.e. 95% CI overlap, PP pairwise comparisons) as described for the SOM model.

2.8. Consumer CSIA-AA mixing model

To determine if CSIA-AA provides a more precise assessment of consumers' use of specific basal energy sources, we first used a 2-way ANOVA (with interaction) to assess the effect of consumer species and habitat on EAA $\delta^{13}C$ values. There were no significant differences for grass shrimp across habitats, but periwinkles in mangrove habitat differed significantly from those in marsh and mixed habitats for all tracers ($p < 0.05$; Table 2). We then incorporated CSIA-AA data into a 5-tracer ($\delta^{13}C_{Ile}$, $\delta^{13}C_{Leu}$, $\delta^{13}C_{Phe}$, $\delta^{13}C_{Thr}$, and $\delta^{13}C_{Val}$) mixing model to estimate the proportional contributions of each basal energy source (*Spartina*, *Avicennia*, the POM proxy, and epiphytic macroalgae) to each consumer group (grass shrimp and periwinkles from marsh, mixed, and mangrove habitat).

A linear discriminant analysis (LDA) indicated that all basal energy sources were isotopically distinct in multivariate space, with a training classification rate of 100% and test classification rate of 97%. LD1 accounted for 56% of between-source variance (Fig. S1 in the Supplement at www.int-res.com/articles/suppl/m729p081_supp.pdf). Even so, we similarly combined

Table 2. Mean ± SD $\delta^{13}C$ values for 5 essential amino acids, namely isoleucine (Ile), leucine (Leu), phenylalanine (Phe), threonine (Thr), and valine (Val), of basal energy sources and consumers. Source values in **bold** were used in the mixing model along with individual consumer estimates. The phytoplankton/particulate organic matter (POM) proxy and epiphytic macroalgae were combined *a posteriori* in the model. *Epiphytic macroalgae values from Moyo et al. (2020)

	Species	Habitat	n	$\delta^{13}C_{Ile}$ (‰)	$\delta^{13}C_{Leu}$ (‰)	$\delta^{13}C_{Phe}$ (‰)	$\delta^{13}C_{Thr}$ (‰)	$\delta^{13}C_{Val}$ (‰)
Basal energy sources	Saltmarsh cordgrass *Spartina alterniflora*	Marsh	3	−13.1 ± 0.8	−22.9 ± 0.1	−15.9 ± 0.8	−4.4 ± 1.4	−17.9 ± 0.6
		Mixed	3	−12.3 ± 1.5	−22.7 ± 1.2	−16.5 ± 1.9	−3.5 ± 3.7	−18.9 ± 0.8
		Total	6	**−12.7 ± 1.1**	**−22.8 ± 0.7**	**−16.2 ± 1.3**	**−3.9 ± 2.5**	**−18.4 ± 0.8**
	Black mangrove *Avicennia germinans*	Mixed	3	−21.2 ± 2.0	−32.0 ± 2.3	−23.9 ± 3.4	−11.8 ± 1.7	−29.1 ± 1.7
		Mangrove	4	−24.5 ± 1.2	−35.4 ± 1.8	−26.0 ± 1.7	−12.0 ± 0.7	−31.4 ± 1.9
		Total	6	**−23.1 ± 2.2**	**−34.0 ± 2.6**	**−25.1 ± 2.6**	**−11.9 ± 1.1**	**−30.4 ± 2.0**
	Ribbed mussel *Geukensia demissa* — POM proxy	Marsh	6	−19.5 ± 1.0	−27.7 ± 0.6	−26.8 ± 0.9	−14.8 ± 1.0	−25.1 ± 0.9
		Mixed	7	−20.2 ± 1.0	−28.0 ± 0.5	−26.9 ± 0.8	−14.4 ± 1.2	−25.8 ± 0.7
		Total	13	**−19.9 ± 1.0**	**−27.8 ± 0.5**	**−26.8 ± 0.8**	**−14.6 ± 1.1**	**−25.5 ± 0.8**
	Epiphytic macroalgae*	Marsh	5	**−23.3 ± 0.7**	**−30.6 ± 0.9**	**−29.5 ± 1.3**	**−17.9 ± 1.1**	**−28.8 ± 1.7**
Consumers	Grass shrimp (*Palaemonetes* spp.)	Marsh	6	−21.7 ± 1.8	−28.2 ± 1.1	−26.4 ± 0.6	−11.4 ± 0.9	−25.5 ± 1.0
		Mixed	6	−21.7 ± 2.1	−28.2 ± 2.4	−26.5 ± 2.2	−12.3 ± 3.2	−25.2 ± 2.8
		Mangrove	7	−20.2 ± 0.9	−27.3 ± 1.5	−25.4 ± 1.2	−10.8 ± 1.8	−24.3 ± 1.8
	Marsh periwinkle snail *Littoraria irrorata*	Marsh	6	−16.0 ± 0.8	−22.9 ± 1.3	−21.3 ± 1.2	−10.3 ± 0.9	−19.9 ± 1.2
		Mixed	6	−16.2 ± 0.9	−23.1 ± 0.6	−21.5 ± 0.5	−9.5 ± 1.3	−20.5 ± 0.7
		Mangrove	6	−22.9 ± 1.6	−29.6 ± 1.0	−27.3 ± 0.6	−17.2 ± 1.3	−27.4 ± 1.2

the POM proxy and epiphytic macroalgae into an 'algae' source *a posteriori* to match the bulk-tissue mixing models. We then used principal component analysis to visualize basal energy source and consumer EAA $\delta^{13}C$ values to ensure that source values fully encapsulated the range of consumer values before applying mixing models (Fig. 2D; Phillips et al. 2014). The first principal component (PC) explained 85.18% of the variation, and all EAA $\delta^{13}C$ loadings on this PC were positive. All basal energy sources were separated, and all consumers fell within their range (Table 2).

We applied a minimal TEF for both consumer species (0.1 ± 0.1‰), as only EAAs were used (McMahon et al. 2010). Model specifications (i.e. number of chains, iterations, burn-in, and thinning) were as described for the SOM model. Additionally, we used the same metrics for evaluating parameter convergence (i.e. Gelman-Rubin diagnostic, posterior predictive distribution) and comparing model outputs within and across habitats (i.e. 95% CI overlap, PP pairwise comparisons) as described for the SOM and bulk-tissue consumer models. We then compared consumer bulk-tissue and CSIA-AA model output 95% CI to evaluate if the results agreed and if CSIA-AA improved estimate precision.

3. RESULTS

3.1. SOM mixing model

When comparing within habitats, we found that *Spartina* and algae were the dominant basal carbon sources contributing to SOM in marsh and mixed habitats (~38–46 and ~43–50%, respectively, Table 3, Fig. 3). While predicted 95% CI overlapped among *Spartina* and algae (Table 3), pairwise comparisons indicated that carbon from *Spartina* comprised a greater proportion of SOM relative to carbon from *Avicennia* (~11–12%) within both marsh (PP = 99.4%) and mixed (PP = 98.6%) habitats (Table S1). In contrast, *Avicennia* replaced *Spartina* as a dominant carbon source to SOM in mangrove habitats (~62 and ~8%, respectively, PP = 97.2%). In marsh and mangrove habitats, predicted algae carbon contributions to SOM (~43 and ~29%, respectively) were higher than those of the non-dominant macrophyte (~11 and ~8%, respectively, Table 3, Fig. 3); however, the certainty of the former was slightly lower than that of the latter (PP = 89.2 vs. 90.4%).

We also found differences in the relative importance of specific basal carbon sources to SOM when comparing across habitats (Table 3, Fig. 3). Specifi-

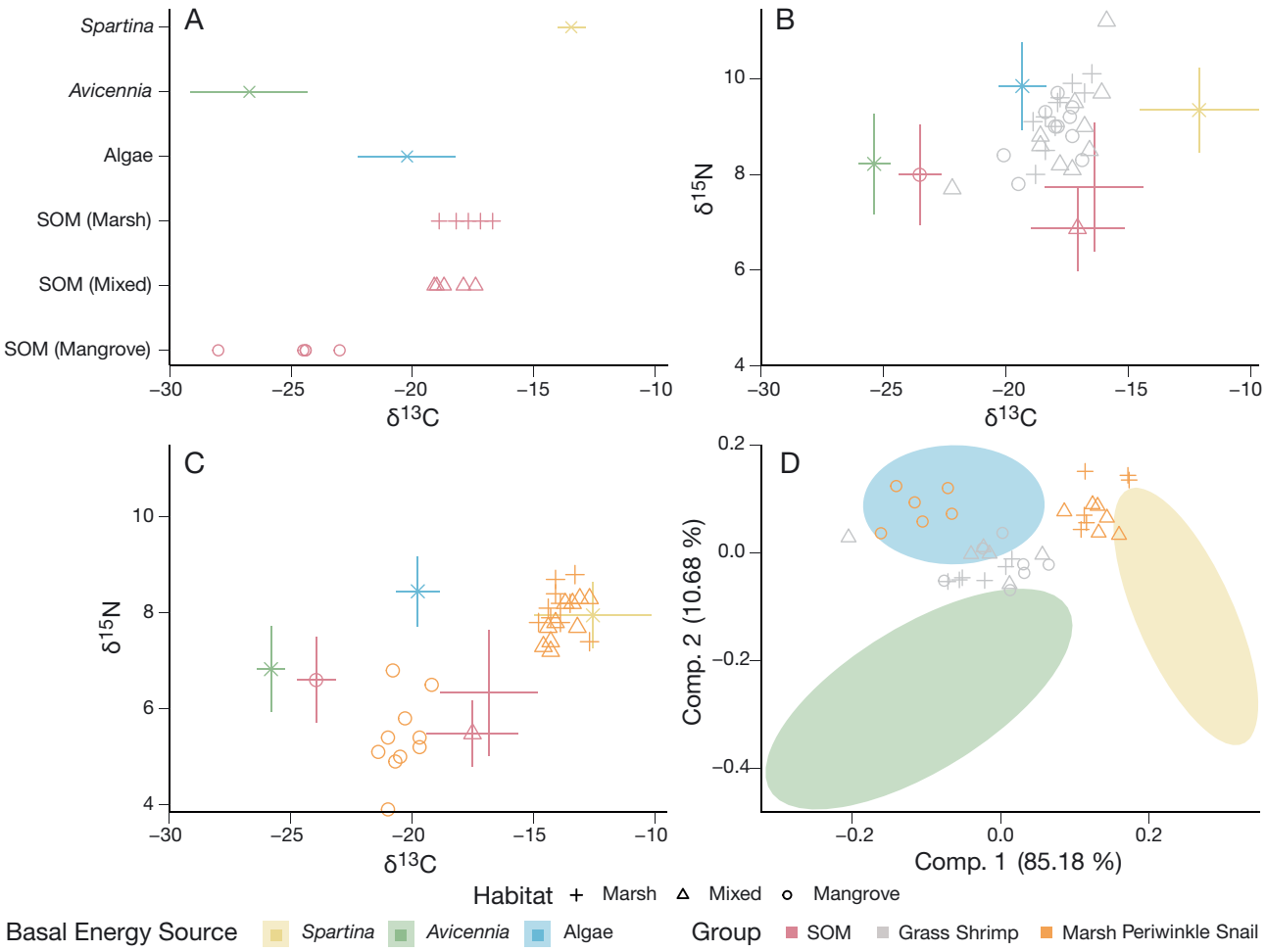

Fig. 2. Isotope values incorporated for (A) soil organic matter (SOM), (B) grass shrimp (*Palaemonetes* spp.), and (C) marsh periwinkle snail *Littoraria irrorata* bulk-tissue stable isotope mixing models. Basal energy sources are plotted as trophic enrichment factor-adjusted means and SD and SOM/consumers are plotted as individual points. (D) Principal components 1 and 2 of principal component analysis on essential amino acid $\delta^{13}C$ values incorporated in the compound-specific stable isotope mixing model. Basal energy sources are plotted as 95% ellipses, and consumers are plotted as individual points. For all plots, colors represent basal energy sources, SOM, and marsh residents, and shapes represent habitats. 'Algae' represents the phytoplankton/particulate organic matter proxy and epiphytic macroalgae combined *a posteriori*

cally, pairwise comparisons indicated that *Spartina* provided more carbon to SOM in marsh (PP = 97.8%) and mixed (PP = 99.1%) habitats relative to SOM in mangrove habitats (Table S2). In addition, *Avicennia* carbon contributed more to SOM in mangrove habitats than it did to SOM in marsh (PP = 97.7%) or mixed (PP = 97.5%) habitats (Table S2). Despite the high uncertainty (i.e. large 95% CI) of algal carbon contributions to SOM, estimates remain consistent across habitats (Table 3, Fig. 3).

3.2. Grass shrimp mixing models

The bulk-tissue SIA models suggested that *Spartina* (~36–40%) and algae (~42–46%) are the dominant basal energy sources supporting grass shrimp food webs within both marsh and mixed habitats (Table 3, Fig. 3). While there is high overlap in bulk-tissue SIA model output 95% CIs between *Spartina* and algae (Table 3), pairwise analyses indicated that both contribute more than *Avicennia* (~18%) to grass shrimp food webs in marsh habitat (PP ⩾ 99.8%) and *Spartina* also contributes more than *Avicennia* (~17%) in mixed habitat (PP = 98.4%; Table S1). In contrast, the bulk-tissue SIA model-predicted contributions of all energy sources to grass shrimp food webs in mangrove habitats broadly overlapped (Table 3; Table S1). The CSIA-AA model agreed that algal sources provide more energy than *Avicennia* within marsh and mixed habitats (PP ⩾ 97.4%; Table 3, Fig. 3) and revealed that algae are the dominant basal energy

Table 3. Median and 95% credible intervals (CI) for the percent contribution of each basal energy source to soil organic matter (SOM) and consumers in marsh, mixed, and mangrove habitat based on bulk-tissue stable isotope analysis (SIA) and compound-specific SIA-amino acid (CSIA-AA) data. 'Algae' includes a phytoplankton/particulate organic matter proxy and epiphytic macroalgae combined *a posteriori*. SOM contributions to aquatic consumers in the bulk models were re-allocated to the other sources based on the SOM mixing model estimates

Method	Group	Habitat	*Spartina*		*Avicennia*		Algae	
			Median (%)	95% CI	Median (%)	95% CI	Median (%)	95% CI
Bulk-tissue SIA	SOM	Marsh	46	20–66	11	2–27	43	11–73
		Mixed	38	15–59	12	2–29	50	15–79
		Mangrove	8	1–28	62	14–86	29	7–74
	Grass shrimp	Marsh	40	21–55	18	6–33	42	16–70
		Mixed	36	14–55	17	4–35	46	14–80
		Mangrove	38	15–54	38	14–59	23	7–64
	Marsh periwinkle snail	Marsh	80	69–87	4	2–9	16	7–28
		Mixed	80	66–89	5	2–10	15	5–29
		Mangrove	13	3–33	32	11–60	53	17–85
CSIA-AA	Grass shrimp	Marsh	12	3–27	9	2–27	79	50–92
		Mixed	11	2–25	14	2–45	73	43–92
		Mangrove	18	8–29	12	2–31	69	48–86
	Marsh periwinkle snail	Marsh	55	47–63	4	1–13	41	29–49
		Mixed	54	48–61	4	1–11	42	33–49
		Mangrove	5	1–12	9	2–21	85	74–93

source for grass shrimp food webs within all habitats (~69–79%, PP ⩾ 97.4%; Table 3, Fig. 3; Table S1).

When comparing individual basal energy source contributions across habitats, the bulk-tissue SIA and CSIA-AA models showed that *Spartina* and algae energetic inputs to grass shrimp food webs did not change across habitats (Table 3, Fig. 3; Table S2). The bulk-tissue SIA models indicated that *Avicennia* contribution is greatest to grass shrimp food webs in mangrove habitat (PP > 92%; Table S2), but the CSIA-AA model estimates of *Avicennia* contribution did not change across habitats (Table 3; Table S2). Nearly all grass shrimp CSIA-AA model output CI ranges were narrower than those produced by the bulk-tissue SIA models (Table 3).

3.3. Periwinkle mixing models

Within habitats, the bulk-tissue SIA and CSIA-AA models both showed that *Spartina* was the dominant energy source supporting periwinkle food webs in marsh and mixed habitats (bulk-tissue SIA: ~80%, CSIA-AA: ~54–55%, $PP_{bulk\text{-}tissue\ SIA} = 100\%$, $PP_{CSIA\text{-}AA} > 96\%$; Table 3, Fig. 3; Table S1). Additionally, algal sources were secondary in energetic importance ($PP_{bulk\text{-}tissue\ SIA} > 97\%$, $PP_{CSIA\text{-}AA} > 99\%$), but the CSIA-AA model estimated higher algae energy inputs within marsh and mixed habitats than the bulk-tissue SIA models (~41–42 vs. ~15–16%, respectively, Table 3, Fig. 3). Within mangrove habitat, the bulk-tissue SIA models indicated that *Spartina* became the least contributing energy source to the periwinkle food web (~13%, PP > 93%), replaced by both *Avicennia* (~32%) and algae (~53%) contributions (Table 3; Table S1). The CSIA-AA model agreed that *Spartina* energy contributions diminished (~5%) and revealed that algae became the dominant energy source to the periwinkle food web in mangrove habitat (~85%, PP = 100%). *Avicennia* contributed minimally to periwinkle food webs (~9%), based on CSIA-AA model predictions.

Across habitats, the bulk-tissue SIA and CSIA-AA models revealed that *Spartina* energy inputs to periwinkle food webs were lowest in mangrove habitat (PP = 100%), and algae inputs were highest in mangrove habitat (PP = 97.3%) relative to marsh and mixed habitats (Table 3, Fig. 3; Table S2). The bulk-tissue SIA models indicated that *Avicennia* contributed most to periwinkle food webs in mangrove habitat relative to marsh and mixed habitats (PP > 99%; Table S2), but the CSIA-AA model output pairwise comparisons were less certain (PP > 81%; Table 3; Table S2). As with grass shrimp, nearly all periwinkle CSIA-AA model output CI ranges were narrower than those from bulk-tissue SIA models (Table 3).

4. DISCUSSION

We examined how shifts in the dominant macrophyte from *Spartina* to *Avicennia* in salt marshes affected the composition of basal carbon sources found

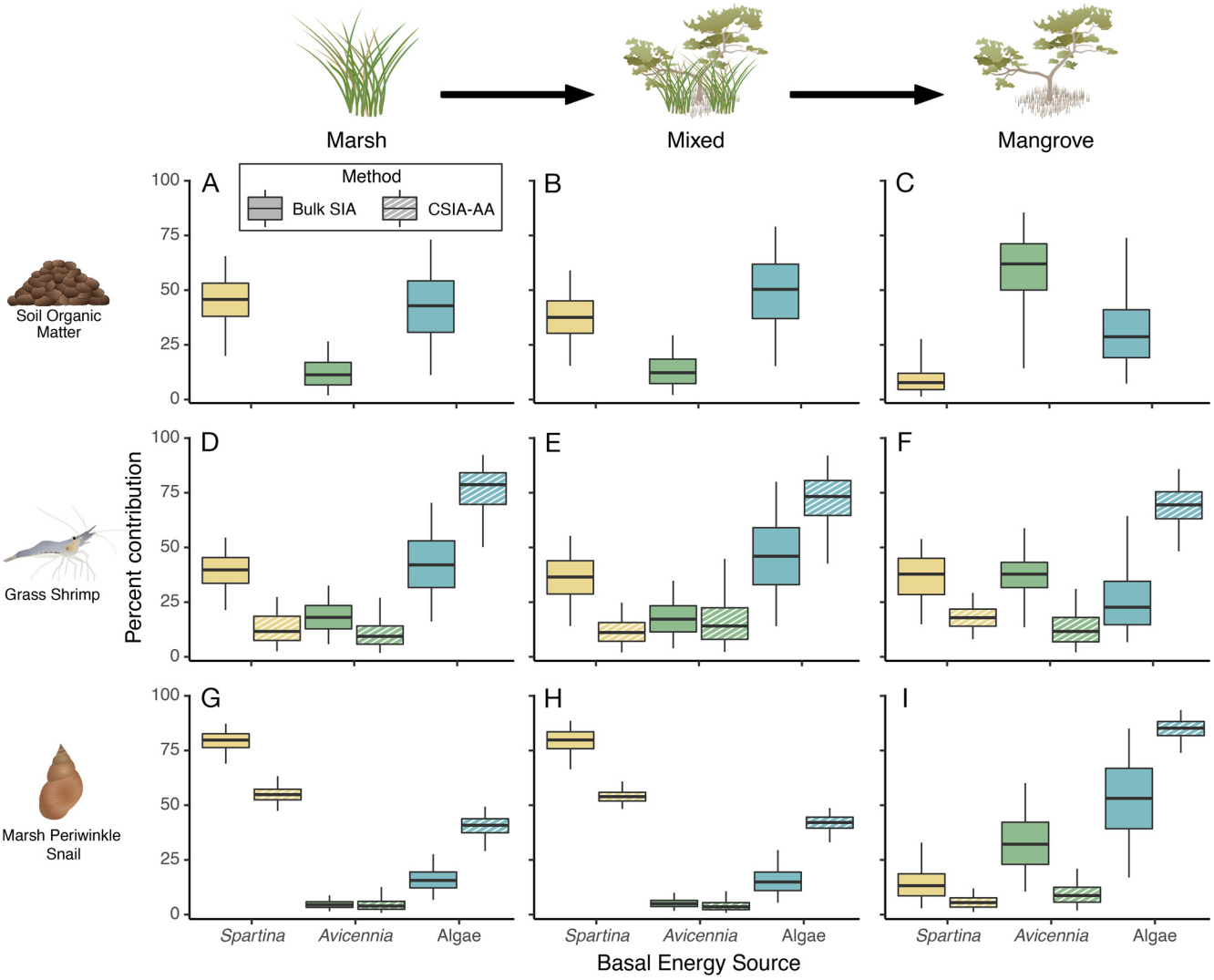

Fig. 3. Estimated basal energy source contributions to (A–C) soil organic matter, (D–F) grass shrimp (*Palaemonetes* spp.), and (G–I) marsh periwinkle snails *Littoraria irrorata* in *Spartina*-dominated (marsh; A,D,G), mixed (B,E,H), and *Avicennia*-dominated (mangrove; C,F,I) habitats. Thick horizontal lines represent the median, boxes extend to the 25th and 75th quartiles, and whiskers encapsulate the 95% credible interval. Colors represent basal energy sources. Box patterning represents stable isotope analysis (SIA) method, with solid boxes representing bulk-tissue SIA mixing model results and striped boxes representing compound-specific SIA-amino acid (CSIA-AA) mixing model results. Iconography is from the Integration and Application Network (ian.umces.edu/media-library)

in SOM and the relative importance of specific basal energy pathways to the food webs supporting 2 common salt marsh resident consumers. Consistent with our hypotheses, we found that the composition of basal carbon sources contributing to SOM across marsh, mixed, and mangrove habitats broadly reflected the transition in dominant macrophyte. In contrast, the basal energy pathways supporting a nektonic grazing consumer (grass shrimp) did not vary across habitats, but those supporting an epibenthic deposit-feeding consumer (periwinkle) did shift along the marsh to mangrove habitat transition. While results using bulk-tissue SIA and CSIA-AA broadly agreed on the patterns of basal energy pathway reliance across habitats, CSIA-AA was able to provide more precise estimates (i.e. narrower CIs) and clarify the relative importance of specific basal energy pathways, such as algal carbon, to salt marsh consumers.

4.1. SOM

The relative composition of basal carbon sources contributing to SOM shifted when transitioning from

marsh to mangrove habitats. This shift indicates that a change in dominant vegetation also alters the detrital pathway, especially when transitioning to complete *Avicennia* dominance, not just co-occurrence. Our results also indicate that the importance of algal carbon to SOM found within marsh and mixed habitats is non-trivial. Specifically, we found it to be similar in contribution to SOM as carbon from *Spartina*, suggesting that these 2 carbon sources may be equally important to the detrital pathway of coastal Louisiana salt marshes and estuarine food webs. Even so, the importance of *Spartina*-derived carbon to SOM highly varied across habitats with differing macrophyte dominance, while algal carbon contributions to SOM were relatively conserved across habitats (evidenced by similar 95% CI and low PP values).

A slight decrease in algal carbon contribution to SOM in mangrove habitats relative to marsh and mixed habitats could be a function of lower algal primary production at this site, as mangroves often occur at higher elevations than *Spartina* (Smee et al. 2017). Regardless, our results suggest a consistent contribution of algal carbon to SOM and through it the potential support of marsh consumers via detrital and/or deposit-feeding pathways. The differences in *Avicennia* carbon contribution to SOM in mixed and mangrove habitats could be a combination of a temporal lag (i.e. how long mangroves have been present at each site, something we were unable to assess in this study) and differences in decomposition rates between *Spartina* and *Avicennia* (i.e. slower decomposition in *Avicennia*). However, the latter hypothesis contrasts with previous findings suggesting that *Avicennia* decomposes faster than *Spartina* (Perry & Mendelssohn 2009, Simpson et al. 2021).

4.2. Grass shrimp

As hypothesized, basal energy pathways supporting grass shrimp food webs were unaffected by shifts in macrophyte dominance across habitats. Isotopic mixing models using bulk-tissue SIA suggested that both *Spartina* and algae were important basal energy sources to grass shrimp food webs within marsh and mixed habitats, but these models had difficulty resolving which basal energy pathways were most important within mangrove habitats. CSIA-AA improved pathway distinctions, clarifying estimated contributions to grass shrimp food webs and revealing the substantial importance of algal energy pathways across habitats irrespective of macrophyte dominance. These results are broadly consistent with previous findings for grass shrimp and other nektonic species in the southeastern USA (Nelson et al. 2019, Baker et al. 2021). As generalist nektonic grazers, grass shrimp forage on diverse resources (McCann et al. 2017), which could make them more resilient or competitive in the face of environmental change (Richmond et al. 2005, Clavel et al. 2011).

Determining whether the algae necessary to support grass shrimp food webs is equally available across these coastal wetland habitats was beyond the scope of this study but has major implications. If algal abundance declines in mangrove habitat, this could result in a decreased carrying capacity for grass shrimp as marsh transitions to mangrove habitat. In support of this possibility, previous work along the Texas coast found that grass shrimp were less abundant and had lower biomass in mangrove habitat than marsh habitat (Smee et al. 2017). Additionally, a study in southeastern Louisiana found that conversion to mangrove habitat decreased energetic benefits to phytoplankton- and/or epiphytic macroalgae-dependent marsh nekton (Harris et al. 2021). Despite having relatively high mobility within the coastal wetland habitat complex (Kneib 2002), grass shrimp can exhibit high site fidelity for specific intertidal creeks on a scale of a few meters (Allen et al. 2015). Therefore, it seems unlikely that grass shrimp will relocate to areas with increased energetic value or increase their foraging range (Allen et al. 2015). As a result, conversion to mangrove habitat could result in declines in grass shrimp abundance.

4.3. Periwinkles

Unlike grass shrimp, the relative importance of specific basal energy pathways to periwinkle food webs varied in response to shifts in macrophyte dominance across habitats. Specifically, periwinkle food webs derived most of their energy from *Spartina* in marsh and mixed habitats, then shifted towards increased algal reliance in mangrove habitat. This provided support for our hypothesis that shifts in the food web pathways supporting epibenthic deposit feeders would reflect concurrent changes in macrophyte dominance.

The periwinkle food web response is likely related to their specialized, deposit-feeding lifestyle, which results in more limited resource availability than mobile nektonic consumers, like grass shrimp (Vaughn & Fisher 1992, McCann et al. 2017). Additionally, their low trophic position (2.00; McCann et al. 2017) indicates that they forage on basal energy sources,

making them more directly impacted by changes in source abundance. Energy pathway contributions to periwinkle food webs at mixed and marsh sites are nearly identical, suggesting that *Spartina* is a preferred energy source (Bärlocher & Newell 1994, Silliman & Newell 2003, Sieg et al. 2013). Interestingly, the importance of *Avicennia* energy pathways to periwinkle food webs remained minimal across habitats, especially according to the CSIA-AA model, despite its apparent inputs to SOM in mangrove habitats. The lack of *Avicennia* contribution to periwinkle food webs could be due to the refractory nature of mangrove tissues (Alongi 1990); periwinkles might ingest but not assimilate mangrove-derived material, as is the case for other *Littoraria* snails common in tropical mangrove systems (Alfaro 2008).

The shift in energy pathways supporting periwinkle food webs towards algal dominance in mangrove habitats indicates that periwinkles are less specialized than expected and can adapt in response to dominant macrophyte shifts. Even so, the energetic quality of compensatory algal pathways in mangrove habitat might be worse than the preferred *Spartina* pathway. To this point, previous work found that periwinkles exhibit optimal growth on a *Spartina* diet (Bärlocher & Newell 1994), so periwinkle abundance and/or biomass might decrease as marsh transitions to mangrove habitat. Additionally, shifting to algae energy pathways could increase or create new competitive interactions with other species reliant on these pathways, which could further alter periwinkle carrying capacity or indirectly alter the carrying capacity of other algal-dependent marsh species.

4.4. Bulk-tissue SIA vs. CSIA-AA

We found that bulk-tissue SIA and CSIA-AA mixing models generally agreed on patterns of food web energy pathway dependence between species and across habitats, with some exceptions including predictions of relatively higher reliance on algal energy pathways using CSIA-AA. As predicted, CSIA-AA models provided more constrained estimates of the importance of specific basal energy sources supporting consumers in each habitat. The discriminatory power of mixing models generally decreases with an increasing number of sources, and is also strongly influenced by the isotopic differences of sources (Phillips et. 2014). The higher number of tracers (5 vs. 2) used in CSIA-AA models allowed for greater separation among basal energy sources contributing to the observed increased interpretive power. This clarifying effect was more prominent in model predictions of the relative importance of basal energy sources supporting grass shrimp than those supporting periwinkles. In addition, CSIA-AA improved the fit of the mixing polygon for periwinkles in mangrove habitat, therefore better adhering to mixing model best practices (Phillips et al. 2014). Additionally, while algal energy sources were consolidated in this study to facilitate methods comparisons, POM and epiphytic macroalgae had distinct CSIA-AA values. This suggests that, unlike bulk-tissue SIA, future studies could employ CSIA-AA to disentangle the relative importance of these 2 algal pathways as well.

Perhaps the most notable strength of a CSIA-AA approach is the minimization of trophic fractionation, especially when incorporating EAAs (McMahon et al. 2010). Mixing models are sensitive to TEFs; chosen values can substantially alter energy pathway contribution estimates (Bond & Diamond 2011). We used the bulk-tissue SIA TEF values employed by Nelson et al. (2019) in a study of nekton in marsh, mixed, and mangrove habitats near Port Fourchon, Louisiana, to facilitate direct comparison between our studies. However, there is inherent uncertainty between actual TEF values experienced by consumers in our study and the assumed TEF values incorporated into bulk-tissue SIA mixing model analyses. Mixing models using EAAs assume a negligible TEF, thus allowing incorporation of some uncertainty into the model without substantially biasing the results with an assumed, and possibly inaccurate, approximation of bulk-tissue isotopic fractionation (McMahon et al. 2010).

4.5. Caveats and considerations

One caveat to consider is that we only included live plant tissues to represent macrophyte pathways. Prior bulk-tissue SIA studies suggest that senesced plant tissues may differ isotopically from live plant tissues (Currin et al. 1995, Bouillon et al. 2008), which would shift the relative position of macrophyte sources to SOM or consumers in the mixing space, potentially changing mixing model-based estimates of macrophyte contributions to SOM carbon and consumer food webs. However, changes in bulk-tissue $\delta^{13}C$ are likely negligible for both *Spartina* and *Avicennia*, while bulk-tissue $\delta^{15}N$ could decrease by up to a few per mil in senesced tissues (Currin et al. 1995, Bouillon et al. 2008). Therefore, as the SOM model only included bulk-tissue $\delta^{13}C$, it is unlikely that this omis-

sion substantially altered our estimates for macrophyte contributions to SOM carbon. Additionally, basal energy sources are fairly similar for bulk-tissue $\delta^{15}N$ (6.1‰ range in means; Table 1) relative to the more pronounced differences in bulk-tissue $\delta^{13}C$ (13.2‰ range in means). It is possible that shifting bulk-tissue $\delta^{15}N$ values for *Spartina* and *Avicennia* could affect the discrimination between basal energy sources, but bulk-tissue $\delta^{13}C$ probably predominantly drives mixing model results, and therefore a shift in bulk-tissue $\delta^{15}N$ is likely of minor concern.

Second, heterotrophic carbon sources (i.e. bacteria and fungi) were not included in our bulk-tissue SIA and CSIA-AA analyses of SOM carbon and consumer energy pathways. This was due in part to an inability to collect representative bacteria or fungi samples at our study sites in sufficient mass and purity to analyze. While these are potential basal energy sources present in the coastal wetland landscape, a recent study suggested that they contribute minimally to coastal wetland deposit-feeder food webs (Harada et al. 2022).

In addition, SOM was included as an energy source in grass shrimp and periwinkle bulk-tissue SIA mixing models but not in their corresponding CSIA-AA models. SOM innately reflects a mixture of basal carbon sources derived from primary producers (i.e. macrophytes, epiphytic macroalgae, microphytobenthos, and phytoplankton), so its estimated contributions to consumer food webs really reflects a combination of other pathways, not a distinct energy source. Given this, we used a novel approach to determine the proportional contributions of these other basal energy sources to SOM (i.e. based on the results of the SOM mixing model) and then used these proportions to reallocate the estimated SOM contributions to consumer food webs to the estimates for these other sources (*Spartina*, *Avicennia*, and algae). This allowed us to directly compare the importance of these 3 basal energy sources in subsidizing salt marsh consumer food webs across bulk-tissue SIA and CSIA-AA methods, as SOM was not analyzed for CSIA-AA in our study given its mixed nature. While our SOM contribution reallocation approach in bulk-tissue SIA models facilitated a more direct methods comparison, it could have introduced some biases to the model results. For example, bulk-tissue SIA models had higher estimates of *Avicennia* food web contributions in mangrove habitat than the CSIA-AA model did, which, while biologically plausible, could also be to some degree an artifact effect of adding the respective proportion of SOM contributions to the *Avicennia* contribution.

Last, we combined algal energy sources after running the mixing models (*a posteriori*), as one was a proxy (ribbed mussel), and therefore the two differed in elemental composition and the trophic step between them and the consumers. However, *a posteriori* combination can create a slight bias toward the combined basal energy source in a Bayesian framework; initially, all sources are weighted with equal likelihoods of contribution, but, by combining 2 of them, that weight is effectively doubled for the resultant combined source (Stock et al. 2018). Combining sources was not strictly necessary for the CSIA-AA analysis; it was mainly performed to maintain a consistent comparison between SIA methods. In addition, we were unable to collect an additional algal source, microphytobenthos, which can be important in supporting salt marsh food webs (Currin et al. 1995, Galván et al. 2008). Creating one 'algal' group helped ameliorate this by serving as a collective representation of all potential pelagic, epiphytic, and benthic algal and cyanobacterial sources present in the system. However, because these algal sources respond to different drivers and may not be incorporated into the food web in the same way, there is some nuance to the potential food web impact of mangrove encroachment that could not be fully parsed apart. Given the importance of algal energy sources (phytoplankton, epiphytic macroalgae, microphytobenthos) with a transition to mangrove habitat and the different substrates (e.g. soil and sediment surfaces, stems and pneumatophores) that support their production, future work would benefit from adopting a CSIA-AA approach and considering the food web contributions of each algal source (phytoplankton, epiphytic macroalgae, and microphytobenthos) separately.

5. CONCLUSIONS

The Gulf of Mexico is expected to be fully tropicalized by the end of this century (Day et al. 2013, Osland et al. 2021, Bardou et al. 2023), facilitating a large-scale transition from *Spartina*- to *Avicennia*-dominated habitat (Rybczyk et al. 2012). *Avicennia* enters the detrital pathway via SOM when it dominates the landscape; however, as seen with previous work on nekton in southeastern Louisiana, it does not meaningfully enter marsh resident aquatic food webs (Nelson et al. 2019). Instead, algal production is most important energetically across species and habitats. Because *Spartina* SOM composition is replaced with *Avicennia* and algae inputs are conserved, *Avicennia* would need to be able to support more algal produc-

tion than *Spartina* to support detrital-mediated salt marsh food webs similarly. Additionally, the shift towards algae reliance in *Avicennia*-dominated habitat indicates decreased energetic pathway diversity for marsh consumers, which could increase competition and decrease overall production. As marsh residents like the species studied here are important prey for fisheries species, such as red drum *Sciaenops ocellatus* and blue crab *Callinectes sapidus* (Heard 1982, Anderson 1985, Schindler et al. 1994, McQuaid 1996), this habitat transition could have cascading adverse consequences on fisheries production. However, as we did not quantify relative abundances, it is not possible for us to fully predict how populations of marsh species will respond to a transition to mangroves. Even so, our study highlights the need to explicitly explore the links between trophic and population dynamics in this system, those in other states (e.g. Texas, Florida), and those in other countries (e.g. Japan, China) facing mangrove encroachment in future studies. As *Avicennia* dominance becomes more widespread, quantifying the relative ability of each macrophyte to support different modes of algal production (e.g. via outwelling nitrogen to phytoplankton, providing substrate for epiphytic macroalgae or microphytobenthos) is a necessary next step in assessing if this macrophyte shift alters the carrying capacity of coastal wetlands for marsh consumers.

Acknowledgements. We thank The Nature Conservancy for access to their land on Grand Isle, Louisiana; Dr. Jimmy Nelson and Dr. Sydney Moyo for access to their data; Tyler Mauney and Angela Stahl for their assistance with isotope analysis; and the Undergraduate Research Opportunities Program (UROP) administered by Louisiana Sea Grant for funding this work. This project was also funded in part by a graduate research assistantship from the Department of Oceanography and Coastal Sciences at Louisiana State University. Sampling for this project was conducted in accordance with a scientific collection permit from the Louisiana Department of Wildlife Fisheries provided to M.M.B. and The Water Institute of the Gulf. Any use of trade, firm, or product names is for descriptive purposes only and does not imply endorsement by the US Government. We thank 3 anonymous journal reviewers and Jill Bourque from the US Geological Survey Wetland and Aquatic Research Center for reviewing earlier drafts.

LITERATURE CITED

Abrantes KG, Barnett A, Baker R, Sheaves M (2015) Habitat-specific food webs and trophic interactions supporting coastal-dependent fishery species: an Australian case study. Rev Fish Biol Fish 25:337–363

Alderson B, Mazumder D, Saintilan N, Zimmerman K, Mulry P (2013) Application of isotope mixing models to discriminate dietary sources over small-scale patches in saltmarsh. Mar Ecol Prog Ser 487:113–122

Alexander JS, Wilson RC, Green WR (2012) A brief history and summary of the effects of river engineering and dams on the Mississippi River system and delta, Circular 1375. US Department of the Interior, US Geological Survey, Reston, VA

Alexander SK (1979) Diet of the periwinkle *Littorina irrorata* in a Louisiana salt marsh. Gulf Res Rep 6:293–295

Alfaro AC (2008) Diet of *Littoraria scabra*, while vertically migrating on mangrove trees: gut content, fatty acid, and stable isotope analyses. Estuar Coast Shelf Sci 79: 718–726

Allen D, Harding J, Stroud K, Yozzo K (2015) Movements and site fidelity of grass shrimp (*Palaemonetes pugio* and *P. vulgaris*) in salt marsh intertidal creeks. Mar Biol 162: 1275–1285

Alongi DM (1990) Effect of mangrove detrital outwelling on nutrient regeneration and oxygen fluxes in coastal sediments of the central Great Barrier Reef lagoon. Estuar Coast Shelf Sci 31:581–598

Anderson GS (1985) Species profiles: Life histories and environmental requirements of coastal fishes and invertebrates (Gulf of Mexico): grass shrimp. USFWS Biol Rep 82(11.35)

Baker R, Abrantes K, Feller IC (2021) Stable isotopes suggest limited role of wetland macrophyte production supporting aquatic food webs across a mangrove–salt marsh ecotone. Estuaries Coasts 44:1619–1627

Bardou R, Osland MJ, Scyphers S, Shepard C and others (2023) Rapidly changing range limits in a warming world: critical data limitations and knowledge gaps for advancing understanding of mangrove range dynamics in the Southeastern USA. Estuar Coast 46:1123–1140

Bärlocher F, Newell S (1994) Growth of the salt marsh periwinkle *Littoraria irrorata* on fungal and cordgrass diets. Mar Biol 118:109–114

Bond AL, Diamond AW (2011) Recent Bayesian stable-isotope mixing models are highly sensitive to variation in discrimination factors. Ecol Appl 21:1017–1023

Bouillon S, Connolly R, Lee S (2008) Organic matter exchange and cycling in mangrove ecosystems: recent insights from stable isotope studies. J Sea Res 59: 44–58

Cavanaugh KC, Kellner JR, Forde AJ, Gruner DS, Parker JD, Rodriguez W, Feller IC (2014) Poleward expansion of mangroves is a threshold response to decreased frequency of extreme cold events. Proc Natl Acad Sci USA 111:723–727

Childers DL, Day JW Jr, Muller RA (1990) Relating climatological forcing to coastal water levels in Louisiana estuaries and the potential importance of El Niño–Southern Oscillation events. Clim Res 1:31–42

Clavel J, Julliard R, Devictor V (2011) Worldwide decline of specialist species: toward a global functional homogenization? Front Ecol Environ 9:222–228

Coastal Protection and Restoration Authority (2015) Coastwide Reference Monitoring System–Wetlands Monitoring Data. Coastal Information Management System (CIMS) database. http://cims.coastal.louisiana.gov

Comeaux RS, Allison MA, Bianchi TS (2012) Mangrove expansion in the Gulf of Mexico with climate change: implications for wetland health and resistance to rising sea levels. Estuar Coast Shelf Sci 96:81–95

Conner WH, Day JW (1987) The ecology of Barataria Basin, Louisiana: an estuarine profile. USFWS Biol Rep 85(7.13), US Department of the Interior, Washington, DC

Currin CA, Newell SY, Paerl HW (1995) The role of standing dead *Spartina alterniflora* and benthic microalgae in salt marsh food webs: considerations based on multiple stable isotope analysis. Mar Ecol Prog Ser 121:99–116

Day JW Jr, Kemp WM, Yáñez-Arancibia A, Crump BC (2012) Estuarine ecology. John Wiley & Sons, Hoboken, NJ

Day JW, Barras J, Kemp GP, Lane RR, Mitsch WJ, Templet PH (2013) Integrated coastal management in the Mississippi Delta: system functioning as the basis of sustainable management. In: Day JW, Yáñez-Arancibia A (eds) Gulf of Mexico origin, waters, and biota, Vol 4: Ecosystem-based management. Texas A&M University Press, College Station, TX, p 93–107

Deegan LA, Garritt RH (1997) Evidence for spatial variability in estuarine food webs. Mar Ecol Prog Ser 147:31–47

Deegan LA, Hughes JE, Rountree RA (2002) Salt marsh ecosystem support of marine transient species. In: Weinstein MP, Kreeger DA (eds) Concepts and controversies in tidal marsh ecology. Kluwer Academic Publishers, New York, NY, p 333–365

Docherty G, Jones V, Evershed RP (2001) Practical and theoretical considerations in the gas chromatography/combustion/isotope ratio mass spectrometry $\delta^{13}C$ analysis of small polyfunctional compounds. Rapid Commun Mass Spectrom 15:730–738

Fagherazzi S, Wiberg PL, Temmerman S, Struyf E, Zhao Y, Raymond PA (2013) Fluxes of water, sediments, and biogeochemical compounds in salt marshes. Ecol Process 2:3

Fleeger J, Carman K, Webb S, Hilbun N, Pace M (1999) Consumption of microalgae by the grass shrimp *Palaemonetes pugio.* J Crustac Biol 19:324–336

Fry B (2006) Stable isotope ecology. Springer, New York, NY

Galván K, Fleeger JW, Fry B (2008) Stable isotope addition reveals dietary importance of phytoplankton and microphytobenthos to saltmarsh infauna. Mar Ecol Prog Ser 359:37–49

Gelman A (2004) Parameterization and Bayesian modeling. J Am Stat Assoc 99:537–545

Gregg CS, Fleeger JW (1998) Grass shrimp *Palaemonetes pugio* predation on sediment-and stem-dwelling meiofauna: field and laboratory experiments. Mar Ecol Prog Ser 175:77–86

Guest MA, Connolly RM (2005) Fine-scale movement and assimilation of carbon in saltmarsh and mangrove habitat by resident animals. Aquat Ecol 38:599–609

Guo H, Zhang Y, Lan Z, Pennings SC (2013) Biotic interactions mediate the expansion of black mangrove (*Avicennia germinans*) into salt marshes under climate change. Glob Change Biol 19:2765–2774

Haines EB (1976) Stable carbon isotope ratios in the biota, soils and tidal water of a Georgia salt marsh. Estuar Coast Mar Sci 4:609–616

Harada Y, Lee SY, Connolly RM, Fry B (2022) Compound-specific isotope analysis of amino acids reveals dependency on grazing rather than detritivory in mangrove food webs. Mar Ecol Prog Ser 681:13–20

Harris JM, James WR, Lesser JS, Doerr JC, Nelson JA (2021) Foundation species shift alters the energetic landscape of marsh nekton. Estuar Coast 44:1671–1680

Heard RW (1982) Guide to common tidal marsh invertebrates of the northeastern Gulf of Mexico. MASGP-79-004. Mississippi Alabama Sea Grant Consortium, Reinbold Lithographing and Printing Company, Booneville, MS

Henriques M, Granadeiro JP, Piersma T, Leão S, Pontes S, Catry T (2021) Assessing the contribution of mangrove carbon and of other basal sources to intertidal flats adjacent to one of the largest West African mangrove forests. Mar Environ Res 169:105331

Hernandez MF, Midway SR, West L, Tillya H, Polito MJ (2021) Stable isotopes track the ontogenetic movement of three commercially important fishes along a coastal Tanzanian seascape. Mar Ecol Prog Ser 670:139–154

Johnson JJ, Olin JA, Polito MJ (2019) A multi-biomarker approach supports the use of compound-specific stable isotope analysis of amino acids to quantify basal carbon source use in a salt marsh consumer. Rapid Commun Mass Spectrom 33:1781–1791

Kim SL, Koch PL (2012) Methods to collect, preserve, and prepare elasmobranch tissues for stable isotope analysis. Environ Biol Fishes 95:53–63

Klink S, Keller AB, Wild AJ, Baumert VL and others (2022) Stable isotopes reveal that fungal residues contribute more to mineral-associated organic matter pools than plant residues. Soil Biol Biochem 168:108634

Kneib R (2002) Salt marsh ecoscapes and production transfers by estuarine nekton in the southeastern United States. In: Weinstein MP, Kreeger DA (eds) Concepts and controversies in tidal marsh ecology. Kluwer Academic Publishers, New York, NY, p 267–291

Kones JK, Soetaert K, van Oevelen D, Owino JO (2009) Are network indices robust indicators of food web functioning? A Monte Carlo approach. Ecol Model 220:370–382

McCann MJ, Able KW, Christian RR, Fodrie FJ and others (2017) Key taxa in food web responses to stressors: the *Deepwater Horizon* oil spill. Front Ecol Environ 15: 142–149

McKee KL, Vervaeke WC (2018) Will fluctuations in salt marsh–mangrove dominance alter vulnerability of a subtropical wetland to sea-level rise? Glob Change Biol 24: 1224–1238

McMahon KW, Fogel ML, Elsdon TS, Thorrold SR (2010) Carbon isotope fractionation of amino acids in fish muscle reflects biosynthesis and isotopic routing from dietary protein. J Anim Ecol 79:1132–1141

McQuaid C (1996) Biology of the gastropod family Littorinidae. II. Role in the ecology of intertidal and shallow marine ecosystems. Oceanogr Mar Biol Annu Rev 34: 263–302

Metges CC, Petzke KJ, Hennig U (1996) Gas chromatography/combustion/isotope ratio mass spectrometric comparison of N-acetyl-and N-pivaloyl amino acid esters to measure ^{15}N isotopic abundances in physiological samples: a pilot study on amino acid synthesis in the upper gastro-intestinal tract of minipigs. J Mass Spectrom 31: 367–376

Moyo S, Olin J, Johnson J, Lopez-Duarte P and others (2020) Southern Louisiana marsh food webs: 2016 amino acid compound-specific stable isotope data. Gulf of Mexico Research Initiative Information and Data Cooperative (GRIIDC), Harte Research Institute, Texas A&M University, Corpus Christi, TX

Nelson JA, Lesser J, James WR, Behringer DP, Furka V, Doerr JC (2019) Food web response to foundation species change in a coastal ecosystem. Food Webs 21:e00125

Osland MJ, Enwright N, Day RH, Doyle TW (2013) Winter climate change and coastal wetland foundation species: salt marshes vs. mangrove forests in the southeastern United States. Glob Change Biol 19:1482–1494

Osland MJ, Day RH, Michot TC (2020) Frequency of extreme freeze events controls the distribution and struc-

ture of black mangroves (*Avicennia germinans*) near their northern range limit in coastal Louisiana. Divers Distrib 26:1366–1382

Osland MJ, Stevens PW, Lamont MM, Brusca RC and others (2021) Tropicalization of temperate ecosystems in North America: the northward range expansion of tropical organisms in response to warming winter temperatures. Glob Change Biol 27:3009–3034

Parnell A (2021) Package 'simmr', Ver 04:5, https://github.com/andrewcparnell/simmr

Perry CL, Mendelssohn IA (2009) Ecosystem effects of expanding populations of *Avicennia germinans* in a Louisiana salt marsh. Wetlands 29:396–406

Phillips DL, Inger R, Bearhop S, Jackson AL and others (2014) Best practices for use of stable isotope mixing models in food-web studies. Can J Zool 92:823–835

Post DM (2002) Using stable isotopes to estimate trophic position: models, methods, and assumptions. Ecology 83: 703–718

R Core Team (2020) R: a language and environment for statistical computing. R Foundation for Statistical Computing, Vienna, https://www.R-project.org/

Reinnicke S, Juchelka D, Steinbeiss S, Meyer A, Hilkert A, Elsner M (2012) Gas chromatography/isotope ratio mass spectrometry of recalcitrant target compounds: performance of different combustion reactors and strategies for standardization. Rapid Commun Mass Spectrom 26: 1053–1060

Richmond C, Breitburg D, Rose K (2005) The role of environmental generalist species in ecosystem function. Ecol Model 188:279–295

Rodrigues E, Cohen MCL, Liu K, Pessenda LCR and others (2021) The effect of global warming on the establishment of mangroves in coastal Louisiana during the Holocene. Geomorphology 381:107648

Rybczyk JM, Day JW Jr, Yanez-Arancibia A, Cowan JH Jr (2012) Global climate change and estuarine systems. In: Day JW Jr, Crump BC, Kemp WM, Yanez-Arancibia A (eds) Estuarine ecology, 2nd edn. John Wiley & Sons, Hoboken, NJ, p 497–518

Scheffel WA, Heck KL, Johnson MW (2018) Tropicalization of the northern Gulf of Mexico: impacts of salt marsh transition to black mangrove dominance on faunal communities. Estuar Coast 41:1193–1205

Schindler DE, Johnson BM, MacKay NA, Bouwes N, Kitchell JF (1994) Crab: snail size-structured interactions and salt marsh predation gradients. Oecologia 97:49–61

Sieg RD, Willey D, Wolfe K, Kubanek J (2013) Multiple chemical defenses produced by *Spartina alterniflora* deter farming snails and their fungal crop. Mar Ecol Prog Ser 488:35–49

Silliman BR, Newell SY (2003) Fungal farming in a snail. Proc Natl Acad Sci USA 100:15643–15648

Simpson LT, Cherry JA, Smith RS, Feller IC (2021) Mangrove encroachment alters decomposition rate in saltmarsh through changes in litter quality. Ecosystems 24:840–854

Smee DL, Sanchez JA, Diskin M, Trettin C (2017) Mangrove expansion into salt marshes alters associated faunal communities. Estuar Coast Shelf Sci 187:306–313

Stock BC, Jackson AL, Ward EJ, Parnell AC, Phillips DL, Semmens BX (2018) Analyzing mixing systems using a new generation of Bayesian tracer mixing models. PeerJ 6:e5096

Sullivan MJ (1982) Similarity of an epiphytic and edaphic diatom community associated with *Spartina alterniflora.* Trans Am Microsc Soc 101:84–90

Treplin M, Pennings SC, Zimmer M (2013) Decomposition of leaf litter in a US saltmarsh is driven by dominant species, not species complementarity. Wetlands 33:83–89

Vaughn CC, Fisher FM (1992) Dispersion of the salt-marsh periwinkle *Littoraria irrorata*: effects of water level, size, and season. Estuaries 15:246–250

Walsh RG, He S, Yarnes CT (2014) Compound-specific $\delta^{13}C$ and $\delta^{15}N$ analysis of amino acids: a rapid, chloroformate-based method for ecological studies. Rapid Commun Mass Spectrom 28:96–108

Welsh BL (1975) The role of grass shrimp, *Palaemonetes pugio*, in a tidal marsh ecosystem. Ecology 56:513–530

Werner RA, Brand WA (2001) Referencing strategies and techniques in stable isotope ratio analysis. Rapid Commun Mass Spectrom 15:501–519

Whiting GJ, McKellar HN Jr, Spurrier JD, Wolaver TG (1989) Nitrogen exchange between a portion of vegetated salt marsh and the adjoining creek. Limnol Oceanogr 34:463–473

Winemiller KO, Akin S, Zeug SC (2007) Production sources and food web structure of a temperate tidal estuary: integration of dietary and stable isotope data. Mar Ecol Prog Ser 343:63–76

Yando ES, Osland MJ, Willis JM, Day RH, Krauss KW, Hester MW (2016) Salt marsh–mangrove ecotones: using structural gradients to investigate the effects of woody plant encroachment on plant–soil interactions and ecosystem carbon pools. J Ecol 104:1020–1031

Editorial responsibility: Erik Kristensen, Odense, Denmark
Reviewed by: L. Pires-Teixeira and 2 anonymous referees

Submitted: July 26, 2023
Accepted: December 1, 2023
Proofs received from author(s): February 13, 2024